Development of a Performance Prediction Method for Centrifugal Compressor Channel Diffusers

Jeong-Seek Kang

Turbomachinery Department, Korea Aerospace Research Institute P.O.Box 113,
Yusung, Daejeon 305-600, Korea

Sung-Kook Cho, Shin-Hyoung Kang*

School of Mechanical and Aerospace Engineering, Seoul National University,
Shinlim-Dong, Kwanak-Gu, Seoul 151-742, Korea

A hybrid performance prediction method is proposed in the present study. A channel diffuser is divided into four subregions: vaneless space, semi-vaneless space, channel, and channel exit region. One-dimensional compressible core flow and boundary layer calculation of each region with an incidence loss model and empirical correlation of residuary pressure recovery coefficient of a channel predict the performance of diffusers. Three channel diffusers are designed and tested for validating the developed prediction method. The pressure distributions from an impeller exit to the channel diffuser exit are measured and discussed for various operating conditions from choke to nearly surge conditions. The strong non-uniform pressure distribution which is caused by impeller-diffuser interaction is obtained over the vaneless and semi-vaneless spaces. The predicted performance shows good agreement with the measured performance of diffusers at a design condition as well as at off-design conditions.

Key Words : Channel Diffuser Performance Prediction, Centrifugal Compressor, Off-Design Performance Prediction, Pressure Distribution

Nomenclature

A	: Area
AS_4	: Throat aspect ratio
B	: Throat blockage
Cp	: Pressure recovery coefficient
D_H	: Hydraulic diameter
f	: Friction coefficient
i	: Incidence angle (degree)
L	: Diffuser length
LC	: Pressure loss coefficient
L/W_4	: Diffuser length to width ratio
m	: Mass flow rate
M	: Mach number
P	: Pressure

P_o	: Total pressure
Pr_{TT}	: Total to total pressure ratio
Pr_{TS}	: Total to static pressure ratio
R	: Radius
Re	: Reynolds number
T	: Temperature
TLE_3	: Diffuser vane leading edge thickness
V	: Velocity
x	: Coordinate of diffuser length
ZD	: Number of diffuser vanes

Greek symbols

α_3	: Diffuser inlet vane angle (degree)
γ	: Ratio of specific heats
τ_w	: Wall shear stress
2ϕ	: Divergence angle of diffuser vane (degree)
2θ	: Divergence angle of diffuser channel (degree)

* Corresponding Author,
  E-mail : kangsh@snu.ac.kr
  TEL : +82-2-880-7113; **FAX** : +82-2-883-0179
  School of Mechanical and Aerospace Engineering,
  Seoul National University Shinlim-Dong, Kwanak-
  Gu, Seoul 151-742, Korea. (Manuscript **Received** July
  25, 2001; **Revised** May 27, 2002)

Subscripts

2 : Impeller exit (diffuser inlet)
3 : Diffuser vane leading edge
4 : Diffuser throat
5 : Diffuser exit

1. Introduction

The centrifugal compressors are widely used in various technical fields, e.g. turbochargers, air suppliers, refrigeration systems, process compressors, small gas turbines, etc. When higher performance and efficiency are required, vaned diffuser is indispensable to achieve high pressure recovery. However, the design and performance prediction methods of vaned diffuser are not well developed.

Flows from the impeller exit to the diffuser vanes are highly three dimensional and unsteady due to interaction between the two components. Detailed flows through an impeller and a diffuser were measured by Krain (1981, 1984) using a L2F. Dawes (1995) investigated the unsteady interaction using an unsteady numerical simulation. Kano et al. (1982) measured the steady pressure distributions in a channel diffuser for wide range of flow rate. Justen et al. (1998) measured an unsteady pressure field in a channel diffuser in design and near surge flow rates using the fast-response pressure transducers and visualized the instantaneous shock configurations at the choke limit. Kang et al. (2000, 2001) investigated the detailed pressure distributions and unsteady characteristics in a diffuser. However, the flow phenomena at the off-design conditions require further study.

There are several parameters affecting the performance of vaned diffuser. Runstadler et al. (1969) suggested that inlet Mach number, Reynolds number, turbulence level, velocity profile shape factor, nonuniform velocity profile, etc. were important parameters for channel performance. Hoffmann and co-workers (1981, 1984, 1988) reported the effects of turbulence intensity and length scale on diffuser performance. Runstadler et al. (1969, 1973, 1975) and Sovran et al. (1967) reported that the throat blockage was one of the most critical parameters affecting channel performance. Because the flows are so complex, the performance is well predicted neither by simple calculation nor by empirical correlation.

In the present study, a hybrid flow loss model through a channel diffuser is obtained by analyzing the experimental data of Runstadler et al. (1969, 1973, 1975) as well as simple one-dimensional core flow and boundary layer calculations. Three channel diffusers are designed and their performances are tested to verify the developed method. Distributions of static pressure over the channel diffuser are also measured for the design, choke, and near surge flow conditions in the present study.

2. Method of Performance Prediction

Figure 1 shows the design parameters of a channel diffuser. The diffuser region from an impeller exit to the diffuser exit is divided into four subregions as shown in Fig. 2; vaneless space from the impeller exit to the leading edge of a vane, semi-vaneless space downstream to the throat, straight channel region and channel exit region. Performances of each subregion are reasonably estimated to have total performance.
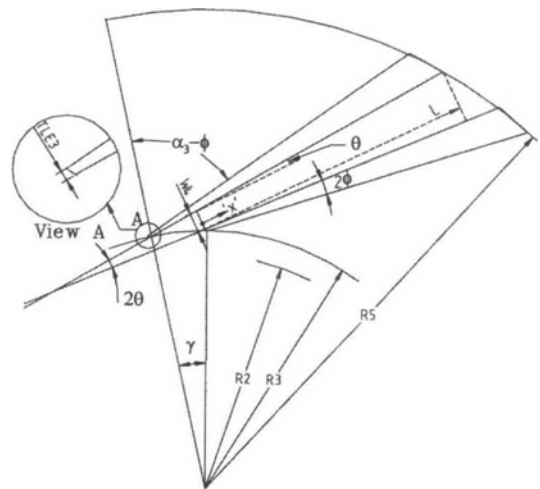

Fig. 1 Configurations and parameters of channel diffuser
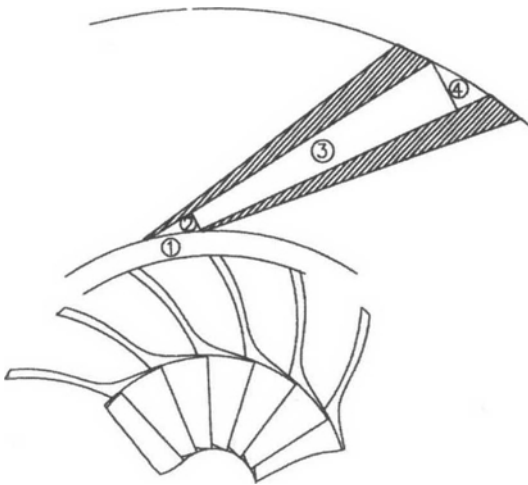
Fig. 2 Division of diffuser into four region (1: vaneless space, 2: semi-vaneless space, 3: channel, 4: channel exit)

The method of Stanitz (1952) is used to calculate the one-dimensional compressible core flow calculation in a vaneless space. The semi-vaneless space is also regarded as a vaneless diffuser with reduced area due to vane thickness. Throat blockage is an important parameter which affects the performance of the channel region (Sovran et al., 1967; Runstadler et al., 1969). From the impeller exit to the throat of channel diffuser, boundary layer is calculated by the method of Walz (1969) to estimate the aerodynamic blockage at the diffuser throat.

The core flow of the channel is calculated by one-dimensional theory of adiabatic frictional flow with variable area and the conceptual sketch is shown in Fig. 3. The momentum equation, continuity equation, perfect gas law and the definition of Mach number produce the following governing Eq. (1):

$$\frac{dM}{M} = -\frac{1+\frac{\gamma-1}{2}M^2}{1-M^2}\frac{dA}{A}$$
$$+\frac{1}{2}\frac{1+\frac{\gamma-1}{2}M^2}{1-M^2}\gamma M^2\frac{4fdx}{D_H} \qquad (1)$$

The relation of stagnation pressure and static pressure, and other adiabatic relations (Saad, 1993) yield Eq. (2):
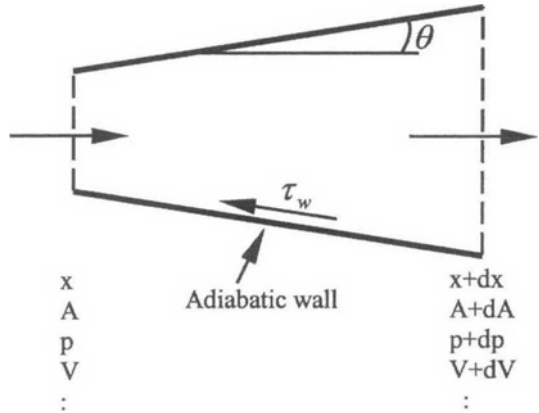

Fig. 3 Core flow model through the channel

$$\frac{dP_0}{P_0} = -\frac{\gamma M^2}{2}\frac{4fdx}{D_H} \qquad (2)$$

According to Eq. (2), stagnation pressure is affected by friction effects but is independent of area change. The results through the channel using Eqs. (1) and (2) with friction coefficient (f) of Karman-Nikuradse relation, Eq. (3), are used for the boundary conditions of boundary layer calculation along the channel wall.

$$\frac{1}{\sqrt{4f}} = 10.8 + 2\log_{10}(\mathrm{Re}\sqrt{4f}) \qquad (3)$$

where Re is Reynolds number. Then core flow and boundary layer calculations are repeated. The friction loss along the channel wall and kinetic energy loss at the channel exit are evaluated by above calculation, which are only part of the whole aerodynamic loss through the channel. The contributions from other sources should be reasonably estimated and added.

The experimental data of Runstadler et al. (1969, 1973, 1975) are available for various channel diffusers. The empirical loss model is obtained to minimize prediction discrepancy. When the calculated pressure coefficients are subtracted from the experimental data, there are residuary coefficients which should be empirically estimated. Figure 4 shows a pressure recovery prediction error when the residuary loss model is applied for the case of $AS_4 = 1.0$. Kang (1998) suggested the following empirical residuary loss model.

$$Cp_{res} = (C_1 + C_2M + C_3B) \times (2\theta) + C_4 + C_5M \\ + C_6M + C_6B + C_7 \log_{10}(AS_4) \quad (4)$$

where $C_1 = 0.0029$, $C_2 = 0.0089$, $C_3 = 0.148$, $C_4 = -0.078$, $C_5 = 0.093$, $C_6 = 0.75$, $C_7 = 0.82$. Figure 5 shows a sample comparison of the predicted pressure recovery coefficients through the channel region by the present method and experimental database for a diffuser (throat aspect ratio of 1.0, throat blockage of 0.02, inlet Mach number of 0.6, and length to width ratio of 16). For small pressure recovery at the channel exit region, an adiabatic frictional flow calculation is performed through the exit region. For a wide range of inlet Mach number from 0.2 to 1.0 and throat blockage from 0.02 to 0.12, the small prediction error in pressure recovery coefficient of 0.011 shows that the residuary loss is modeled well. The other cases (Kang, 1998) for wide range of throat aspect ratio also show good coincidence between the predictions and the measured database of Runstadler et al. (1969, 1973). The last loss-generating source remained is the incidence angle at the vane leading edge for off-design flow rates. The total pressure loss due to the incidence angle is modeled from the experimental data and will be discussed later.
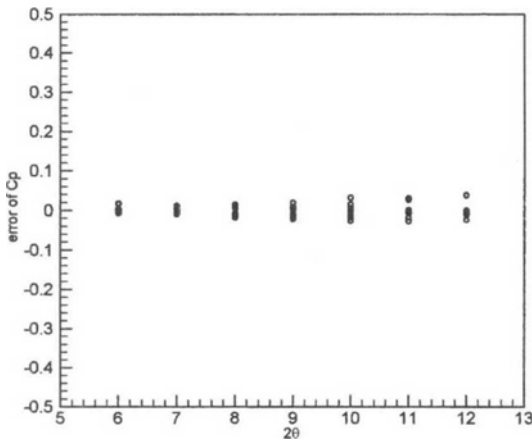
3. Experimental Facility and Instrumentation

Three diffusers are designed and their performances are evaluated with a single stage centrifugal compressor. The high-speed compressor test rig is composed of an impeller, a diffuser, a large collector with four outlet pipes, an inlet settling chamber, a radial turbine, and an instrumentation system (Kang et al., 2000, 2001). The schematic view of the centrifugal compressor test facility is shown in Fig. 6. The radial turbine is driven by compressed air supply. The inlet and outlet total temperatures are measured using the T-type thermocouples installed at the settling chamber and the collector. The rotating speed of

Fig. 4 Pressure recovery prediction error $(AS_4 = 1.0,$ Inlet $M = 0.2, 0.6, 1.0,$ Blockage $= 0.02, 0.06, 0.12,$ mean error $= 0.011)$
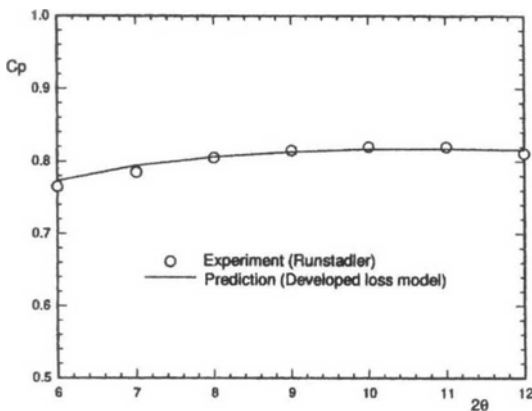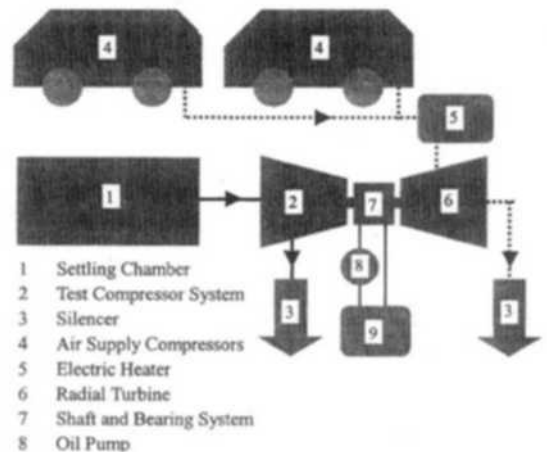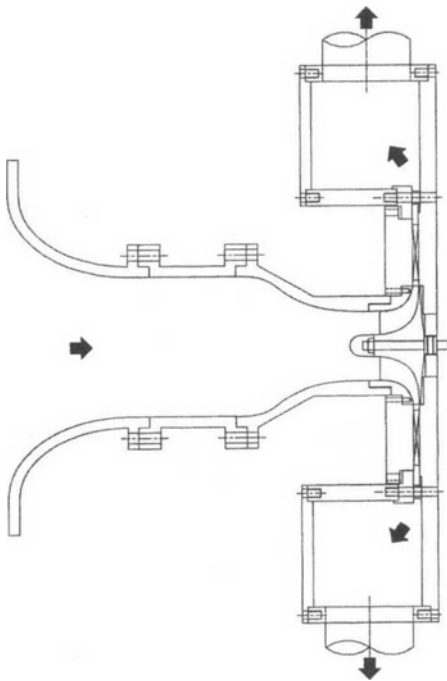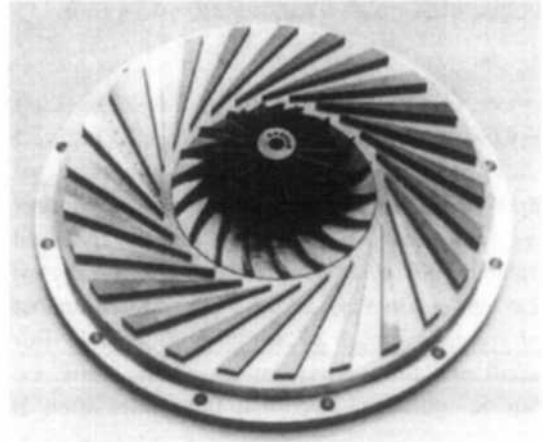
Fig. 5 Pressure recovery prediction of channel by developed loss model $(AS_4 = 1.0,$ Throat blockage $= 0.02,$ Inlet $M = 0.6,$ $L/W_4 = 16)$

1   Settling Chamber
2   Test Compressor System
3   Silencer
4   Air Supply Compressors
5   Electric Heater
6   Radial Turbine
7   Shaft and Bearing System
8   Oil Pump

Fig. 6 Schematic view of compressor test facility

Table 1   Specifications of test impeller

Impeller diameter	110 mm
Inducer tip diameter	63.4 mm
Inducer hub diameter	20.4 mm
Inducer tip blade angle	−60.0 deg.
Inducer hub blade angle	−29.2 deg
Backsweep angle	−35.0 deg. (from radial)
Number of blades	18
Design speed	60,000 rpm
Impeller tip width	5.5 mm

Table 2   Specifications of three test channel diffusers

	Channel 1	Channel 2	Channel 3
L/W_4	11.4	8.35	14
AS_4	1.0	0.765	1.21
2θ (deg)	7.6	7.0	7.0
ZD	25	19	29
θ (deg)	3.4	5.97	2.71
α_3 (deg)	70	70	70
R_3/R_2	1.1	1.1	1.1
TLE_3 (mm)	0.5	0.5	0.5

Fig. 8   Impeller and test channel diffuser 1

the impeller is measured by an induced electro-magnetic force signal between the coil and a permanent magnet fixed on the turbine shaft. The meridional view of the test section is shown in Fig. 7. The specifications of the impeller and three test diffusers are shown in Table 1 and 2.

The test impeller and channel diffuser 1 are shown in Fig. 8 and the three channel diffusers are shown in Fig. 9. The steady pressure distributions in the diffuser 1 are measured at 121 pressure taps of diameter 0.5 mm as shown in Fig. 10. The measured uncertainties are 0.51 % in mass flow rate and 0.35 % in static pressure ratio by the method of Kline et al. (1953).

4. Measured Performance and Pressure Distributions

4.1 Performance

A steady compressor performance was obtained for full range of flow rate from choking to surge conditions using time-averaged static pressures at the channel and impeller exit as shown in Fig. 11. The compressor characteristics show positive slope near the surge condition and negative slope at the other flow rates. The pressure recovery through the diffuser shows its maximum value near the design condition and gradually decreases at the off-design conditions. The pressure at the exit of channel diffuser decreases near the choking
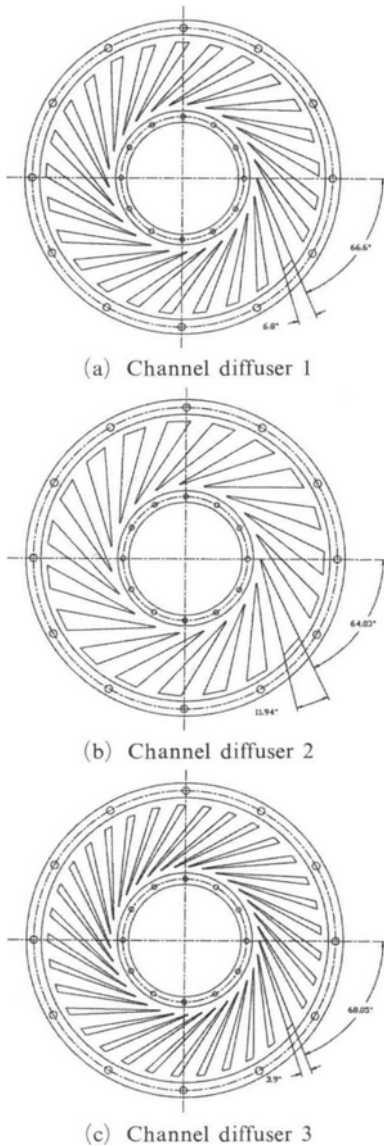

Fig. 7   Meridional view of tested impeller and diffuser

(a) Channel diffuser 1

(b) Channel diffuser 2

(c) Channel diffuser 3
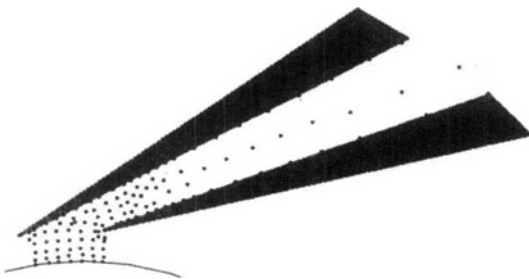
Fig. 9 Three test channel diffusers

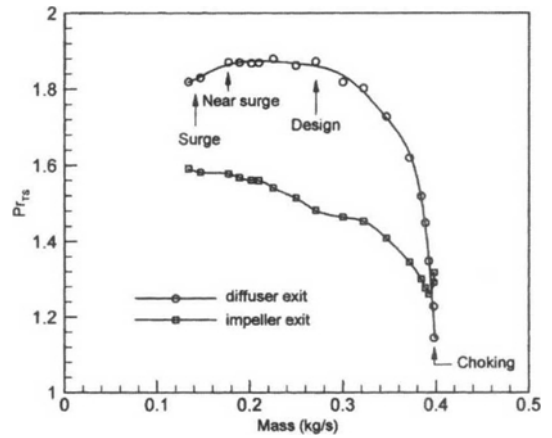**Fig. 10** Location of static pressure taps in the diffuser (channel 1)

Fig. 11 Performance map of compressor at 60,000 rpm (Channel diffuser 1)

condition, however, impeller exit pressure rather increases, which is due to a normal shock in the diffusers (Kang et al., 2000, 2001). The impeller exit pressure becomes higher than the diffuser exit pressure and the diffuser no longer works as a diffuser but as a convergent-divergent nozzle at choking conditions.

4.2 Pressure Distributions

Figure 12 shows the static pressure distributions in a vaneless space. Circumferentially non-uniform pressure distributions are observed in the vaneless space due to high pressure at the leading edge where the flow stagnates. The high pressure vane leading edge of a vane strongly influences the pressure field in the vaneless and semi-vaneless space. The pressure level is lower and more uniform between the vanes afthough higher near the vane location. The pressure non-uniformity caused by the vane leading edge decreases at the vaneless space and the pressures at the impeller exit are fairly uniform and does not show much variation between the pressure side and suction side. The pressure gradient is larger in the pressure side than in the suction side. For near surge flow rate, the pressure gradient in the vaneless and semi-vaneless space is lower than that for the design flow condition as shown in Fig. 12(b). Figure 13 shows the pressure distribution at choke condition where normal shock
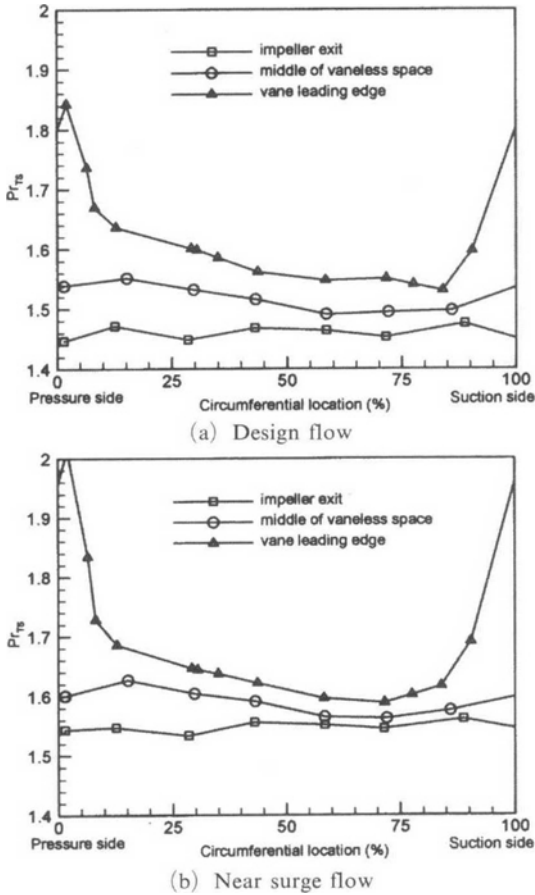
(a) Design flow

(b) Near surge flow

Fig. 12 Pressure distribution in the vaneless space of diffuser 1
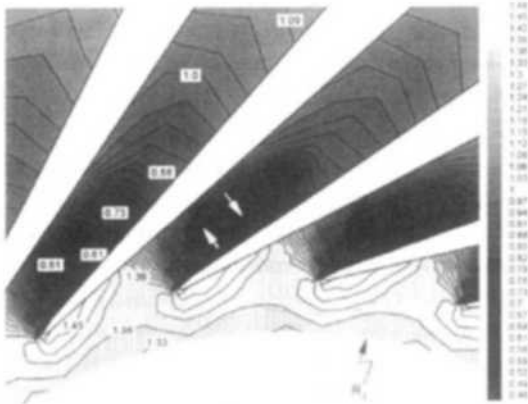

Fig. 13 Time-averaged pressure contour in diffuser 1 at choke condition (Kang et al., 2001)

occurs downstream of throat (Kang et al., 2001). The pressure distributions along the vane
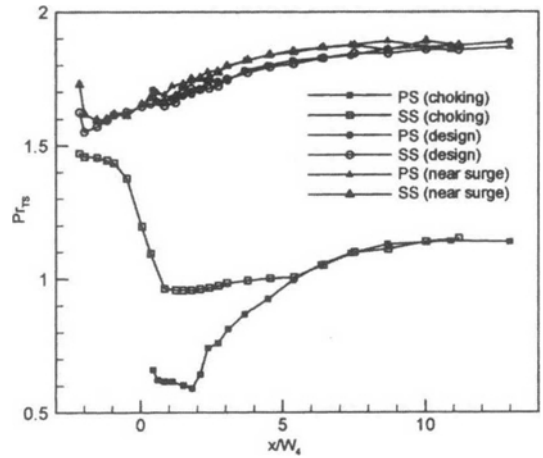

Fig. 14 Pressure variations along the channel for three flow rates in channel 1 (PS : Pressure side, SS : Suction side)

surfaces are shown in Fig. 14. Most of the pressure recovery occurs at the entry of diffuser and the pressure gradient gradually decreases towards downstream. At the design and near surge conditions, the pressure gradually increases from the entry to the exit. Pressure difference between the pressure and suction sides is small. However, at the choke condition, large pressure difference appears between the pressure and suction sides of the vane leading edge and extends to the downstream of shock location. The pressure on both sides converges at the location where x/W_4 is about 5.3.

5. Prediction of Performance

The pressure recovery coefficient of the channel diffusers is estimated using the reference dynamic pressure measured at the impeller exit with the parallel wall vaneless diffuser. The performance of the vaneless diffuser is regarded as a reference (Yoshinaga et al., 1980). R_{exit}/R_2 of the parallel wall vaneless diffuser is 2.0 and tip clearance is 0.3 mm. The impeller exit flow for the design condition is as follows ; $m=0.268$ kg/s, $Pr_{TT}=2.18$, $Pr_{TS}=1.57$, $M_2=0.69$, $\alpha_2=70.3$ deg., $T_2=350.3$ K, where m is mass flow rate, Pr_{TT} the total to total pressure ratio at the impeller exit, Pr_{TS} the total to static pressure ratio at the impeller exit,
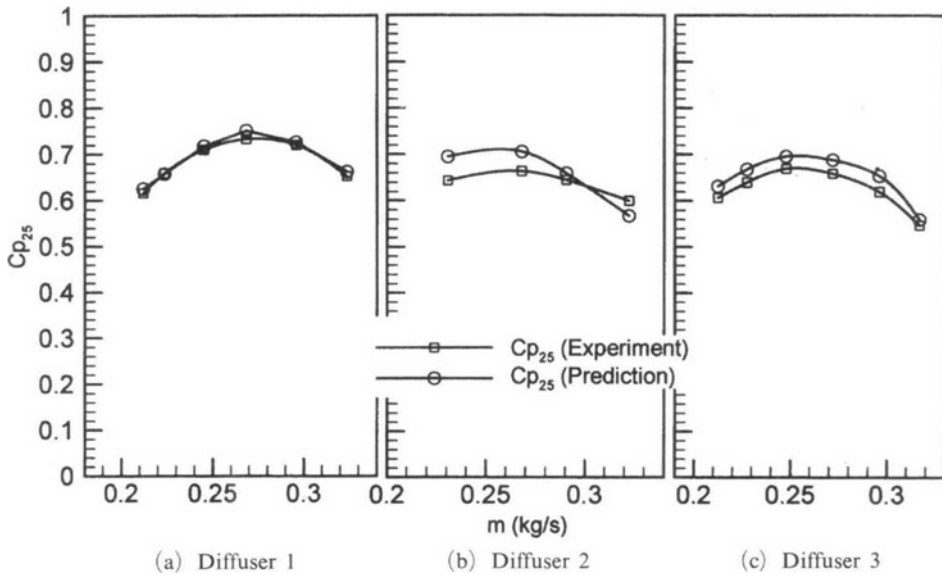
Fig. 15 Comparison of measured and predicted pressure recovery coefficients

M_2 the impeller exit Mach number, α_2 the flow angle at impeller exit, and T_2 the temperature at impeller exit. Since the value of pressure at the impeller exit hub side is slightly higher than that of the shroud side, the mean values of both sides are used as the reference static pressure at the impeller exit. Pressure recovery coefficient is defined as follows:

$$Cp_{25} = (p_5 - p_2) / (p_{02} - p_2) \qquad (5)$$

At design flow rate, the pressure recovery coefficient of channel diffuser 1, 2 and 3 are 0.733, 0.664, and 0.661 and that of the vaneless diffuser is 0.572. The diffuser 1 shows the maximum pressure recovery at the design condition among them. Modeling shows low blockage and low friction loss for throat aspect ratio of 1.0. This result coincides with the experimental results of Runstadler et al. (1969, 1973) and Bhinder et al. (1983).

The incidence loss which is the important component for off-design performance prediction is modeled as follows:

$$LC = 0.005 i^2 \qquad (6)$$

where i is the incidence angle (vane angle–flow angle) of negative value. The coefficient is determined using the measured pressure of the dif-

fusers. It is assumed that there is no incidence loss if i is positive (less than 5 degree) where flow from the impeller exit is accelerated to the diffuser throat. The flow angle is estimated by one-dimensional flow calculation from the inlet to the throat. This model is valid for incidence angle, $-10 < i < 5$.

Figure 15 shows the measured and predicted pressure recovery coefficients for three channel diffusers. There is a good coincidence for the diffuser 1 not only at the design condition but also at the off-design conditions. The results for channel 2 and 3 are also satisfactory.

6. Conclusion

A hybrid channel diffuser performance prediction method using four loss models–friction loss, incidence loss, blockage and complex flow loss, exit kinetic energy loss–is developed in the present study. Friction loss and exit kinetic energy loss are obtained from calculation, while incidence loss and blockage and complex flow loss are obtained from the experimental data. Throat blockage which strongly affects the performance of channel is calculated through a boundary layer calculation. Incidence loss for off-design

conditions is modeled from the measured data. Three channel diffusers are designed and their performances are tested to verify the developed method. The detail distributions of time-averaged pressure over a channel diffuser are measured. Strong non-uniform pressure distributions over the vaneless space and semi-vaneless space are obtained due to high pressure at the vane leading edge. This performance prediction method uses both experimental data and computational results, so it is named as a hybrid method. The predicted performance shows a good coincidence with the experimentally evaluated performance of the channel diffusers at the off-design conditions as well as at the design condition.

Acknowledgment

References

Bhinder, F. S. and Al-Modafar, M. H., 1983, "Development and Application of a Performance Prediction Method for Straight Rectangular Diffusers," *ASME Journal of Engineering for Power*, Vol. 105, pp. 120~124.

Dawes, W. N., 1995, "A Simulation of the Unsteady Interaction of a Centrifugal Impeller with its Vaned Diffuser : Flow Analysis," *ASME Journal of Turbomachinery*, Vol. 117, pp. 213~222.

Hoffmann, J. A., 1981, "Effects of Free-Stream Turbulence on Diffuser Performance," *ASME Journal of Fluids Engineering*, Vol. 103, pp. 385~390.

Hoffmann, J. A. and Fang, L. W., 1988, "Influence of the Structure of Inlet Free-Stream Turbulence on Diffuser Performance," *AIAA Paper* No. 88-3673-CP.

Hoffmann, J. A. and Gonzales, G., 1984, "Effects of Small-Scale, High Intensity Turbulence on Flow in a Two-Dimensional Diffuser," *ASME Journal of Fluids Engineering*, Vol. 106, pp. 121~124.

Justen, F., Ziegler, K. U. and Gallus, H. E.,

1998, "Experimental Investigation of Unsteady Flow Phenomena in a Centrifugal Compressor Vaned Diffuser of Variable Geometry," *ASME Paper* No. 98-GT-368.

Kang, J. S., 1998, *A Study on the Design and Performance Prediction of Centrifugal Compressor Channel Diffuser*, M. S. thesis, Seoul National University, Korea.

Kang, J. S., Cho, S. K. and Kang, S. H., 2000, "Unsteady Flow Phenomena in a Centrifugal Compressor Channel Diffuser," *ASME Paper* No. 2000-GT-451.

Kang, J. S. and Kang, S. H., 2001, "A Study on Pressure Distributions in a Centrifugal Compressor Channel Diffuser," *Trans. of KSME*, Vol. 25, No. 4, pp. 507~513.

Kang, S. H., Kang, J. S. and Cho, S. K., 1998, "A Hybrid Method of Performance Prediction for Channel Diffusers," *Proceedings of the Fourth KSME-JSME Fluids Engineering Conference*, pp. 105~108.

Kano, F., Tazawa, N. and Fukao, Y., 1982, "Aerodynamic Performance of Large Centrifugal Compressors," *ASME Journal of Engineering for Power*, Vol. 104, Oct., pp. 796~804.

Kline, S. J. and McClintock, F. A., 1953, "Describing Uncertainties in Single Sample Experiments," *Mechanical Engineering*, January.

Krain, H., 1981, "A Study on Centrifugal Impeller and Diffuser Flow," *ASME Journal of Engineering for Power*, Vol. 103, pp. 688~697.

Krain, H., 1984, "Experimental Observations of the Flow in Impellers and Diffusers," VKI Lecture Series, 1984-07.

Runstadler, P. W. and Dean, R. C., 1969, "Straight Channel Diffuser Performance at High Inlet Mach Numbers," *ASME Journal of Basic Engineering*, Vol. 91, No. 4 September, pp. 397~422.

Runstadler, P. W., Jr. and Dolan, F. X., 1973, "Further Data on the Pressure Recovery Performance of Straight-Channel, Plane-Divergence Diffusers at High Subsonic Mach Numbers," *ASME Journal of Fluids Engineering*, 73-FE-5.

Runstadler, P. W., Jr., Dolan, F. X. and Dean, R. C., Jr., 1975, *Diffuser Data Book*, Creare, TN-186.

Saad, M. A., 1993, *Compressible Fluid Flow*, 2nd ed., Prentice-Hall, pp. 199~232.

Sovran, G. and Klomp, E. D., 1965, "Experimentally Determined Optimum Geometries for Rectilinear Diffusers with Rectangular, Conical or Annular Cross-section," Fluid Machanics of Internal Flow, General Motors Research Laboratories, Warren, Mich.

Stanitz, J. D., 1952, "One-Dimensional Compressible Flow in a Vaneless Diffusers of Radial and Mixed Flow Centrifugal Compressors, Including Effects of Friction, Heat Transfer and Area Change," NACA TN 2610.

Walz, A., 1969, *Boundary Layers of Flow and Temperature*, Cambridge : M. I. T. Press.

Yoshinaga, Y., Gyobu, I., Mishina, H., Koseki, F. and Nishida, H., 1980, "Aerodynamic Performance of a Centrifugal Compressor with Vaned Diffusers," *ASME Journal of Fluids Engineering*, Vol. 102, pp. 486~493.